IMPACT OF AN EDGE RESONANT TRANSPORT LAYER ON FAST-ION CONFINEMENT IN THE ASDEX UPGRADE TOKAMAK

J.GALDON-QUIROGA[1,2], M.GARCIA-MUNOZ[2], S.SHARAPOV[3], L.SANCHIS-SANCHEZ[2], L.CHEN[4], M.DUNNE[1], J.GONZALEZ-MARTIN[2], M.HOELZL[1], A.S.JACOBSEN[1], K.G.MCCLEMENTS[3], M.NOCENTE[5], F.ORAIN[1], J.F.RIVERO-RODRIGUEZ[2], D.A.RYAN[3], M.SALEWSKI[6], P.SCHNEIDER[1] A.SNICKER[7], W.SUTTROP[1], Y.TODO[8], M.A.VAN ZEELAND[9], E.VIEZZER[2], M.WILLENSDORFER[1], D.ZARZOSO[10], F.ZONCA[4,11], THE ASDEX UPGRADE[1] AND MST1 TEAMS*

[1]Max Planck Institute for Plasma Physics, 85748 Garching, Germany
[2]Department of Atomic, Molecular and Nuclear Physics, University of Seville, Seville, Spain
[3]CCFE Culham Science Centre, Abingdon OX14 3DB, United Kingdom
[4]IFTS, Zhejiang University, 310027, Hangzhou, China
[5]Dipartimento di Fisica G'Occhialini, University of Milano Bicocca, Milano, Italy
[6]Department of Physics, Technical University of Denmark, Kgs. Lyngby, Denmark
[7]Department of Applied Physics, Aalto University, FI-00076, Aalto, Finland
[8]National Institute for Fusion Science, Toki, Japan
[9]General Atomics, San Diego, California, 92186-5608, United States
[10]Laboratoire PIIM, Aix-Marseille University, France
[11]ENEA C.R., 65-00044, Frascati, Italy
*See the author list of *H. Meyer et al 2017 Nucl. Fusion **57** 102014*

Email of corresponding author: joaquin.galdon@ipp.mpg.de // jgaldon@us.es

Abstract

An edge resonant transport layer has been found to explain many aspects of fast-ion confinement under symmetry breaking 3D edge perturbations, such as edge localized modes (ELMs) and externally applied magnetic perturbations (MPs). Experimental measurements in the ASDEX Upgrade (AUG) tokamak show that fast-ion losses in the presence of symmetry breaking 3D fields strongly depend on the poloidal spectra of the applied MPs. This fast-ion transport is explained in terms of a resonant interaction between the perturbative fields and the particle orbital frequencies, which leads to the build-up of an Edge Resonant Transport Layer (ERTL) in the vicinity of the separatrix. Full-orbit following simulations including the plasma response have been performed to characterize the ERTL by means of the variation in the particle toroidal canonical momentum. The combination of the poloidal spectra of the applied MPs and the relative phase of the particles with respect to the perturbation determines the radial direction of the fast-ion transport, therefore degrading or improving the fast-ion confinement. Consequently, an appropriate arrangement of the heating systems and externally applied 3D fields provides an excellent tool to tailor the fast-ion distribution, thus modifying the drive/damping of electromagnetic instabilities through local wave-particle interactions. In this regard, proof-of-principle experiments have been conducted in AUG, where NBI-driven toroidal Alfvén eigenmodes (TAEs) were excited and suppressed on command using this technique.

The importance of the ERTL is extended to ELM-induced fast-ion losses, during which acceleration of beam ions has been recently observed in AUG. Multiple velocity-space structures are observed to vary with the beam source and q_{95} values. This suggests that the acceleration results again from a resonant interaction between the beam ions and parallel electric fields arising during ELM filament eruption.

The experimental results presented here may shed light on the physics underlying fast-ion confinement in the presence of both self-generated and imposed edge 3D perturbations. In the case of externally applied MPs, experiments have demonstrated the possibility of actuating on limited phase-space volumes of the fast-ion distribution to actively control TAEs, which is of great interest for future burning plasma experiments like ITER.

1. INTRODUCTION

Edge localized modes (ELMs) are plasma instabilities closely linked to high-confinement operational regimes in magnetically confined fusion devices. The large transient heat and particle losses that occur during type-I ELMs are thought to be intolerable for the plasma facing components of future burning plasma experiments [1,2]. Thus, the suppression – or at least the mitigation - of ELMs is mandatory. One of the most investigated techniques is ELM control through the application of externally applied magnetic perturbations (MPs) [3]. The application of externally applied MPs have been proven to successfully mitigate and suppress ELMs in several machines [4-6], and the plasma response has been found to play an important role in determining the field perturbation amplitude [7-10]. However, a deleterious effect is observed on the confinement of fast-ions due to

both non-axisymmetric perturbations: externally applied MPs [11-14] and ELMs [11], although on different time-scales.

In the paper, a candidate mechanism to explain the fast-ion transport and loss in the presence of 3D fields is presented, which is based on a resonant interaction between the fast-ion orbits and the perturbation. In the case of externally applied MPs, it is found that a number of geometrical resonances appear in a region of 5 cm within the separatrix – the so called Edge Resonant Transport Layer (ERTL) – which gets activated in the presence of 3D perturbations [15]. Section 2 describes full-orbit simulations carried out with the ASCOT code in the presence of externally applied MPs. These numerical simulations have been compared to experiments conducted at ASDEX Upgrade and are supported by analytical calculation of linear and non-linear resonances. It is found that the radial direction of the particle transport strongly depends on both, the poloidal spectrum of the applied perturbation and the relative toroidal phase between the perturbation and the neutral beam injection (NBI). In section 3, experiments carried out at ASDEX Upgrade aiming at controlling NBI-driven Alfvén Eigenmodes [16] are described. A clear effect on the AE stability was observed, depending on the poloidal spectrum of the applied perturbation, and leading to the mitigation, suppression or even drive of TAEs [17]. On the other hand, section 4 describes the acceleration of beam ions during ELMs which has been reported for the first time in the ASDEX Upgrade tokamak [18] through the measurement of ELM induced fast-ion losses. The acceleration mechanism is proposed to be a resonant interaction between the fast-ions and the parallel electric fields emerging during the ELM crash. Full-orbit following simulations, including a simple analytical model for the 3D parallel electric fields, reveal resonant structures similar to those appearing in the case of fast-ion transport induced by externally imposed 3D fields. Finally, the results are discussed in section 5 and some conclusions are drawn.

2. THE FAST ION EDGE RESONANT TRANSPORT LAYER

Experiments have been carried out in the ASDEX Upgrade tokamak (AUG) to investigate the effect of externally applied 3D magnetic perturbations on fast-ion confinement. There was particular interest in the dependence of fast-ion losses on the poloidal spectra of the applied perturbation, which also affects the plasma response [15]. In AUG two sets of 8 MP coils – one above and one below the midplane – are installed, providing considerable flexibility in the configuration of the applied perturbation. In these experiments a magnetic perturbation with a dominant toroidal mode number of n=2 was applied in low collisionality deuterium plasmas ($\upsilon^* = 0.2$). 5 MW of NBI power were applied from two different NBI sources with a primary injection energies of 93 keV and 60 keV. In order to scan the poloidal spectrum of the applied MPs, a continuous differential phase ($\Delta\phi_{ul}$) scan was carried out. In the experiment this was done by keeping constant the current flowing through the lower set of coils while varying the current flowing through the upper set of coils with a slow frequency of 2 Hz. The fast-ion losses are monitored through the measurements of a scintillator based fast-ion loss detector (FILD) located at the midplane. The measurements are illustrated in Figure 1. The differential phase scan of the MPs modulates the density pump-out and fast-ion losses (a), in blue and black respectively, and also the ELM size (b).

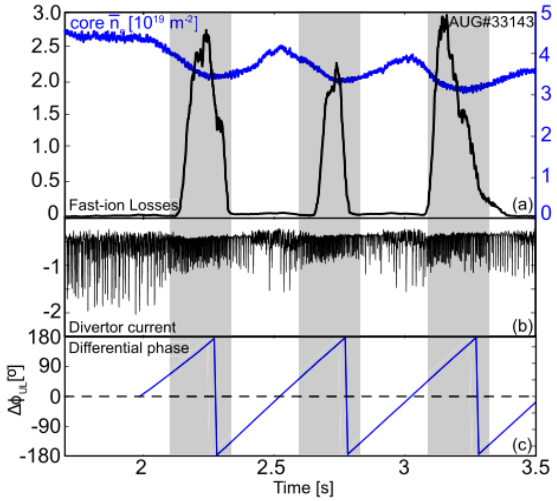

Figure 1: (a) Temporal evolution of the plasma density (blue) and normalized fast-ion losses (black). (b) Divertor current signal, which is used as an ELM monitor. (c) Differential phase between the upper and the lower set of MP coils. The time intervals where fast-ion losses are observed are highlighted in grey. [15]

In order to investigate the effect of externally applied 3D perturbation fields on fast-ion confinement, full orbit following simulations have been carried out with the ASCOT code [19]. The perturbed fields were calculated with the single fluid MHD code MARS-F [20]. In the simulations, a scan was performed in the particles' initial radial position (from 1.9 to 2.2 m) and energy (from 20 to 100 keV). The particles were started at Z=0 m and with a pitch of $\Lambda = \frac{v_{||}}{v} = -0.5$ (where $v_{||}$ is taken with respect to the magnetic field and therefore being co-going particles since I_p and B_t are antiparallel in these experiments), approximately corresponding to the NBI injection angle at the low-field side. The transport is studied in terms of the variation of the toroidal canonical angular momentum ($P_\phi = mRv_\phi - Ze\psi$), which is a motion invariant in axisymmetric systems. A positive (negative) variation of P_ϕ is related to an inwards (outwards) radial transport of the particle.

The results of the simulations are shown in Figure 2, where (a) corresponds to a case with $\Delta\phi_{ul} = 40^o$ and (b) corresponds to a case with $\Delta\phi_{ul} = -100^o$. Blue-black (Yellow-white) regions correspond to an outward (inward) radial transport of the particles. It can be observed that most of the transport is located in a region of ~5 cm around the separatrix. In the case of $\Delta\phi_{ul} = 40^o$ (a) mainly an outward transport of the particles is observed. However, in the case of $\Delta\phi_{ul} = -100^o$ (b) an inward transport of the particles is observed. This indicates that the differential phase of the applied MP has an effect on the direction of the associated particle transport.

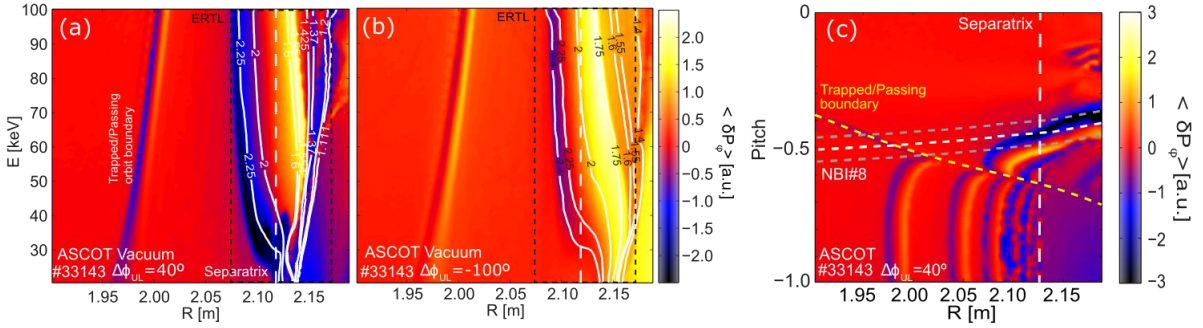

Figure 2: (a) and (b) show a contour plot of the variation of the toroidal canonical angular momentum (P_ϕ) as a function of the particles' initial radial position and energy. An initial pitch of Λ= -0.5 was selected for this simulation. (a) $\Delta\phi_{ul}$=40º and (b) $\Delta\phi_{ul}$= -100º. The blue-black regions correspond to an outward radial transport of the particles, while the yellow-white regions correspond to an inward radial transport of the particles. The white lines indicate rational contours of ω_b/ω_d which fulfill the resonance condition. The separatrix is indicated by a dashed white line for reference. (c) shows the variation of P_ϕ as a function of the particle initial radial position and pitch. Particles were launched with an energy of 60 keV. The deposition of NBI source 8 is indicated for reference and the trapped passing boundary is also highlighted [15]

This transport can be explained in terms of a resonant interaction between the particle orbits and the perturbation. Particles that are in phase with the perturbation are subject to radial transport. In general, the condition for a particle to be in resonance with a perturbation can be derived analytically by applying a projection of the perturbation into the particle's motion [20]. If the particle's motion is considered to be unperturbed, the linear resonance condition is derived. If the particle's motion is considered to be perturbed, then the non-linear resonance condition is obtained. In this case, for trapped particle orbits, the non-linear resonance condition is given by [13]:

$$\frac{\omega_b}{\bar{\omega}_d} = \frac{n(1+l)}{p_0(1+l)+p'}$$

where ω_b is the bounce frequency, $\bar{\omega}_d$ is the toroidal precessional frequency, and n, l, p_0 and p' take integer values being: n the toroidal mode number, l the non-linear harmonic, p_0 the primary bounce harmonic and $p = p_0 + p'$ is the non-linear bounce harmonic. In these plots, the white lines correspond to iso-values of the ratio $\omega_b/\bar{\omega}_d$ which fulfill the resonance condition for different values of l, p_0 and p'. It can be observed that these resonance lines overlap with the regions of large values $|\delta P_\phi|$, thus suggesting that a resonant mechanism is responsible for this kind of transport.

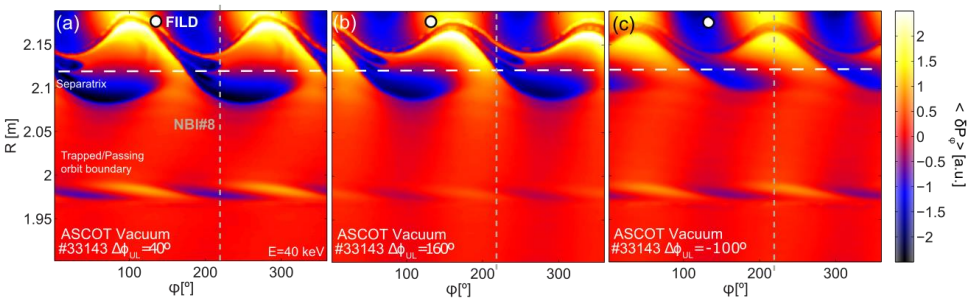

Figure 3: Contour plot of the variation of toroidal canonical angular momentum (P_ϕ) as a function of the particles' initial radial and toroidal position. A pitch of 0.5 and energy of 40 keV was used in these simulations. The approximate birth position of NBI fast-ions is indicated by a green dashed line, while the position of the FILD is indicated by a white circle. [15]

Additional simulations have been carried out in which a scan in the initial particle radial and toroidal position was performed, while keeping the same initial energy and pitch angle. The results are shown in Figure 3, where the toroidal injection angle of the NBI system is indicated by a green dashed line and the FILD position is indicated by a white circle. Plots (a), (b) and (c) show the results for different $\Delta\phi_{ul}$ of 40º, 160º and -100º respectively. It can be observed that varying the differential phase between the MP coils can change the direction of the transport of the particles that are being deposited by the NBI at a fixed toroidal position. Additionally, it can also be seen that the variation of P_ϕ shows a periodic behavior in the toroidal direction. This indicates that the problem is twofold, and suggests that the confinement of the NBI ions could be improved by an advantageous arrangement of both the poloidal spectrum of the perturbation – in practice, the differential phase between the upper and lower set of coils – and the relative toroidal phase between the NBI injection and the MP configuration.

3. APPLICATION TO ALFVÉN ACTIVITY CONTROL

In light of these results, experiments were carried out in AUG aiming at controlling the Alfvén activity driven by NBI fast-ions. The idea is that the application of the externally applied MPs could be used to remove/fill specific regions of the fast-ion phase-space which are responsible for the drive of the Alfvén waves [17]. In order to drive TAEs unstable using NBI fast-ions during the current flattop at AUG, the experiment was carried out in a low density plasma $n_e \lesssim 4 \cdot 10^{-19}\, m^{-3}$ with an elevated q_{95}~7 and applying 5 MW of NBI power [16]. In the experiment, first, a continuous differential phase scan was carried out in this scenario to identify the phases producing the maximum and minimum FILD signal, similar to the experiment described in Section 2. Then, two different shots were carried out in which the MPs were applied intermittently with two differential phases corresponding to the maximum ($\Delta\phi_{max}$) and minimum ($\Delta\phi_{min}$) level of fast-ion losses measured by FILD. The results of the experiment are shown in Figure 4. Figures (a) and (b) show the spectrograms obtained from a magnetic pick-up coil, while (c) shows the modulation of the FILD signal in both cases. The white timetraces indicate the time windows in which the MPs are applied. TAEs with frequencies between 70-120 kHz are observed. A clear modulation of the TAE activity is observed correlated with the application of the MPs. In the case in which $\Delta\phi_{max}$ is applied (a), the TAEs are mitigated until t=3.0s; afterwards, the TAEs are suppressed. This time point coincides with a change from an on-axis to an off-axis NBI source. On the other hand, in the case in which $\Delta\phi_{min}$ is used (b), the TAEs are driven unstable when the MPs are applied. Figure (c) shows how the modulation of the fast-ion loss level measured by FILD is larger in the $\Delta\phi_{max}$ case.

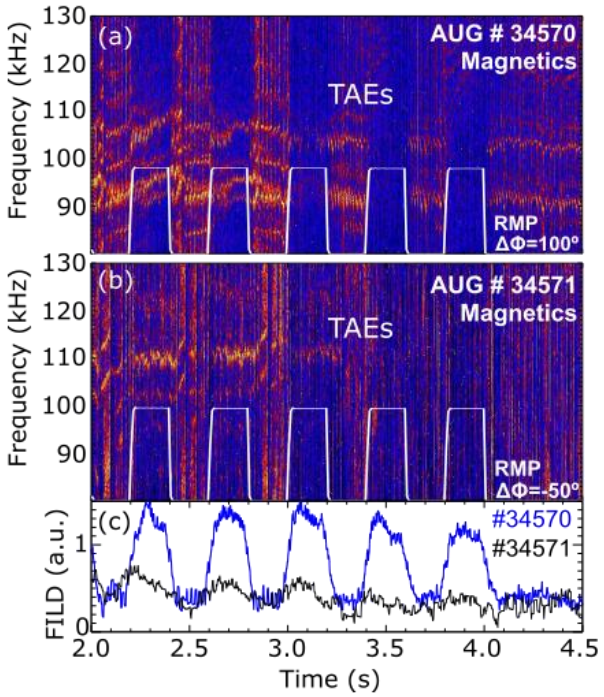

Figure 4: Modulation of the NBI driven TAE activity by means of the externally applied MPs in AUG. (a) and (b) show magnetics spectrograms corresponding to two different shots with different $\Delta\phi$ of the applied MP. (c) shows the modulation of the fast-ion loss level obtained with the FILD diagnostic. [17]

In order to gain a better understanding of the experiment, full-orbit following simulations were carried out with ASCOT for three different cases: one in an axisymmetric magnetic equilibrium, and two including the MPs and associated plasma responses at $\Delta\phi_{ul} = 100^o$ and $\Delta\phi_{ul} = -50^o$. The particles were followed during 10 ms. The resulting radial fast-ion profiles are shown in Figure 5. In (a) the radial profile integrated over the whole pitch angle range is plotted, while in (b) only the particles with pitch between $v_{||}/v = 0.7$ and 0.8 are taken into account. It can be seen that in the case where a maximum level of fast-ion losses is expected ($\Delta\phi_{ul} = 100^o$), the radial profile is below the axisymmetric case, which we use for reference. On the contrary, in the case in which a lower level of fast-ion losses is expected ($\Delta\phi_{ul} = -50^o$), the difference between this and the axisymmetric case is smaller at $\rho_{pol} > 0.8$, while a slight increase of the fast-ion population is observed at $\rho_{pol} < 0.8$. Ongoing work is focused on the modelling of the NBI driven TAEs using the non-linear hybrid kinetic-MHD code MEGA, including the perturbed magnetic field configuration, in order to assess the extent to which the effect on the TAE stability is due to a redistribution of the fast-ion population in phase-space which impacts the drive of the modes.

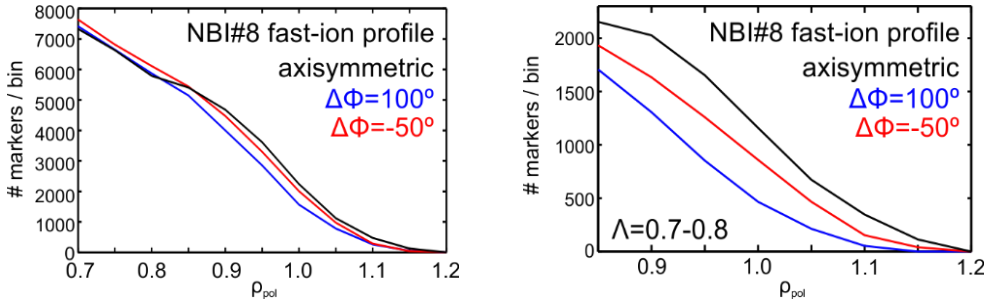

Figure 5: Radial fast ion profile simulated with ASCOT for three different cases: axisymmetric (black), $\Delta\phi_{ul} = 100^o$ (blue) and $\Delta\phi_{ul} = -50^o$ (red). (a) shows the radial profile integrated over all pitch angles, while (b) shows the same quantity but in a limited range of pitch angles, where the effect of the MP coils is expected to be larger. [17]

4. OBSERVATION OF BEAM ION ACCELERATION DURING EDGE LOCALIZED MODES

Fast-ion losses induced by ELMs are also observed in ASDEX Upgrade by means of FILD detectors. The timetraces of these losses exhibit a filamentary-like behavior, showing multiple spikes in the FILD signal – so called fast-ion filaments - for a single ELM crash [11,18]. Differences are observed in the signals measured by two FILD detectors located at the same poloidal position, but different toroidal position, thus revealing the 3D nature of the phenomenon. In recent experiments, a population of fast-ions, with energies well above the primary NBI injection value, has been detected correlated with the application of NBI and the occurrence of ELMs [18]. The experiments were carried out in low collisionality plasmas with NBI being the only source of fast-ions to the plasma. This is illustrated in Figure 6, where (a) shows the velocity-space measured by FILD during an ELM crash, (b) shows a tomographic inversion of the measurement, and (c) shows the synthetic FILD signal recovered from the tomography. In (a), two main populations at pitch angles of $\arccos(-\frac{v_{||}}{v}) \sim 45^o$ and $\sim 60^o$ are observed, which correspond to first orbit losses of NBI sources 7 and 8 respectively. For each of these populations, different spots can be identified: the main one, at r_L~4.1 cm which corresponds to the primary energy of the NBI system; a second one, at r_L~2.9 cm, which corresponds to the half-energy of the NBI system; and, more interestingly, an additional spot at $r_L > 5$ cm – a high-energy feature - which corresponds to energies well above the primary NBI injection value. The high energy feature is correlated with the application of the NBI and the occurrence of ELMs. It has a pitch angle structure which varies with q_{95}. However, the velocity-space measurement of FILD has a finite resolution in pitch angle and energy, meaning that the measurement is a distortion of the velocity-space distribution of lost fast-ions which are reaching the detector pinhole [22]. In order to overcome this limitation, the undistorted velocity-space measurement can be retrieved by means of tomographic inversion techniques, taking into account the response of the detector. This is shown in (b), revealing that the high-energy feature is well localized in energy. In (c) the synthetic FILD signal obtained from the tomographic inverted distribution is shown for completeness. It can be seen that there is a good agreement with the experimental signal.

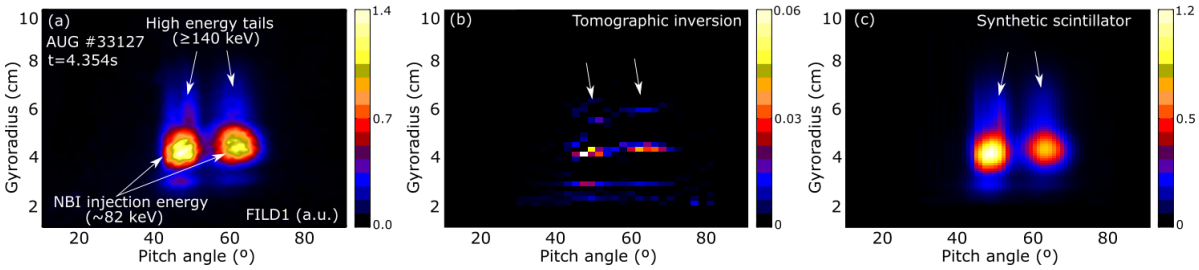

Figure 6: (a) Velocity-space measurement from FILD of beam-ion losses during an ELM. A population of beam-ions with energies well above the main NBI injection is observed. (b) Tomographic inversion of the FILD signal, showing the undistorted velocity-space measurement where the detector response has been taken into account. (c) Synthetic FILD signal after applying a forward model to the inverted measurement. Good agreement is observed with the experimental signal. [23].

The acceleration mechanism leading to the high-energy feature is proposed to be a resonant interaction between the fast-ions and the parallel electric fields emerging during the ELM crash. In order to investigate the ELM induced fast-ion transport and beam-ion acceleration, two different kinds of simulations have been carried out, results from which are shown in Figure 7. In the first case, simulations including only the magnetic field perturbation during the ELM, provided by the non-linear resistive MHD code JOREK [24] have been carried out with ASCOT. The results are shown in Figure 7 (a). In these simulations, a scan was performed in the initial radial position and pitch angle of the particles. The transport of the particles is again evaluated through the variation of the toroidal canonical angular momentum, as described in Section 2. Secondly, additional simulations have been carried out with only a parallel electric field superimposed with the equilibrium field, in a realistic AUG axisymmetric configuration. The parallel electric field is implemented through a simple analytical model which encapsulates the 3D character of the perturbation:

$$\vec{E} = \overrightarrow{b_{||}} \cdot A \cdot exp\left[\frac{(\rho - \rho_0)^2}{2\sigma^2}\right] \cos(n\phi - m\theta^* + \alpha)$$

where $\overrightarrow{b_{||}}$ is a unit vector parallel to the magnetic field, A is a parameter controlling the intensity of the electric field, ρ_0 is the radial position of the perturbation, σ is a parameter controlling the radial width of the perturbation, ϕ is the toroidal angle, θ^* is the poloidal angle, α is the phase of the perturbation, and n and m are

the toroidal and poloidal mode numbers respectively. In this case the parameters of the parallel electric field model were set to $A = 2.0$ kV/m, $\rho_0 = 0.9$, $\sigma = 0.1$, $n = 10$ and $m = q \cdot n$, and the particles were followed for 50 μs. The results are shown in Figure 7 (b), where again the energy gain of the particles is shown as a function of the initial radial position and pitch angle. The energy gains obtained are of the order of tens of keV, consistent with the FILD measurements. In both cases we observe resonant-like structures which are different for passing (clear vertical structures in the plot) and trapped orbits. These features are similar to those of the ERTL for the fast-ion transport in the presence of externally applied MPs, shown in Figure 2 (c).

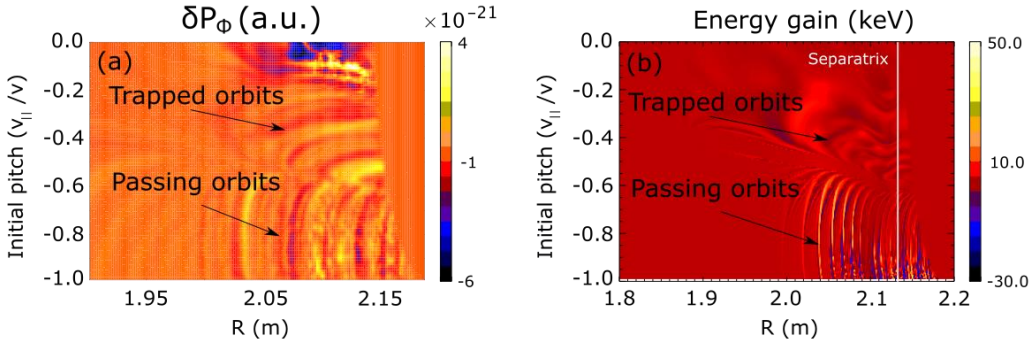

Figure 7: Full-orbit following simulations of beam-ions. (a) Simulation including only the magnetic field perturbation provided by JOREK. The variation of toroidal canonical angular momentum is shown as a function of the initial particle radial position and pitch. (b) Simulation including only a parallel electric field as provided by a simple analytical model. The energy gain is shown as a function of the initial particle radial position and pitch. Similar resonant structures can be observed in (a) and (b). [18,23]

5. CONCLUSIONS

Experiments at AUG have shown that fast-ion losses in the presence of externally applied MPs strongly depend on the poloidal spectrum of the applied perturbation. The fast-ion transport is explained in terms of a resonant interaction between the fast-ion orbits and the 3D perturbation. Orbit following simulations reveal the existence of an edge resonant transport layer (ERTL) in a region of few cm around the separatrix, where the variation of toroidal canonical angular momentum is used as a proxy for radial transport of the particles. The numerical results are supported by analytical calculation of linear and non-linear resonances. These simulations indicate that the radial direction of the fast-ion transport is determined by both the poloidal spectrum of the perturbation and the relative toroidal phase between the perturbation and the fast-ion deposition profile. Therefore, an appropriate arrangement of the heating systems together with the MP coil configuration provides an excellent tool to tailor the fast-ion distribution, thus modifying the drive/damping of electromagnetic instabilities through local wave-particle interactions. In this regard, proof-of-principle experiments have been carried out in AUG, where the stability of NBI driven TAEs was shown to be affected using this technique. Depending on the poloidal spectrum of the applied perturbations, TAEs were observed to be mitigated, suppressed or excited. These results open the door towards the possibility of using MP coils as a tool to control AE activity by actuating on limited phase-space volumes of the fast-ion distribution.

The concept of the ERTL has been extended to the study of ELM induced fast-ion losses, during which acceleration of beam ions has been recently measured by means of fast-ion loss detectors in AUG. A resonant interaction between the beam ion orbits and the parallel electric fields emerging during ELM filament eruption has been proposed as a possible mechanism to explain the beam-ion acceleration. Full-orbit following simulations have revealed features that are analogous to those observed in the case of externally applied MPs. Resonant structures are observed in simulations including only the perturbed magnetic fields, and separately in simulations including only the parallel electric field through an analytical 3D model. A topological difference between passing and trapped particles is observed.

The experimental results presented here may contribute to a better understanding of the physics underlying fast-ion confinement in the presence of both self-generated and imposed edge 3D perturbations.

ACKNOWLEDGEMENTS

This work has been carried out within the framework of the EUROfusion Consortium and has received funding from the Euratom research and training programme 2014-2018 under grant agreement No 633053. The views and opinions expressed herein do not necessarily reflect those of the European Commission.

REFERENCES

[1] LEONARD, A.W., Phys. Plasmas 21, 090501 (2014)
[2] EICH, T. et al., Nucl. Mater. Energy 12, 84-90 (2017)
[3] LOARTE, A. et al., Nat. Physics 2, 369 (2006)
[4] EVANS, T. et al., Phys. Rev. Lett. 92, 235003 (2004)
[5] JEON, Y.M. et al., Phys. Rev. Lett. 109, 035004 (2012)
[6] SUTTROP, W. et al., Nucl. Fusion 58, 096031 (2018)
[7] PAZ-SOLDAN, C. et al., Phys. Rev. Lett. 114, 105001 (2015)
[8] NAZIKIAN, R. et al., Phys. Rev. Lett. 114, 105002 (2015)
[9] KIRK, A. et al., Nucl. Fusion 55, 043011 (2015)
[10] ORAIN, F. et al., Nucl. Fusion 57, 022013 (2017)
[11] GARCIA-MUNOZ, M. et al., Plasma Phys. Control. Fusion 55, 124014 (2013)
[12] VAN ZEELAND, M et al., Nucl. Fusion 55, 073028 (2015)
[13] MCCLEMENTS, K.G. et al., Plasma Phys. Control. Fusion 57, 075003 (2015)
[14] GARCIA-MUNOZ, M. et al., IAEA FEC Conference Proceedings 2016
[15] SANCHIS-SANCHEZ, L. et al., submitted to Plasma Phys. Control. Fusion (2018)
[16] GEIGER, B. et al., EPS Conference Proceedings 2018
[17] GARCIA-MUNOZ, M. et al., submitted to Plasma Phys. Control. Fusion (2018)
[18] GALDON-QUIROGA, J. et al., Phys. Rev. Lett. 121, 025002 (2018)
[19] HIRVIJOKI, E. et al., Comput. Phys. Commun. 185, 1310 (2014)
[20] LIU, Y. et al., Plasma Phys. Control. Fusion 52, 104002 (2010)
[21] ZONCA, F. et al., New J. Phys. 17, 013052 (2015)
[22] GALDON-QUIROGA, J. et al., Plasma Phys. Control. Fusion 60, 105005 (2018)
[23] GALDON-QUIROGA, J. et al., EPS Conference Proceedings 2018
[24] HOELZL, M. et el., Physics of Plasmas 19, 082505 (2012)